An autologous dendritic cell vaccine promotes anticancer immunity in ovarian cancer patients with low mutational burden and cold tumors

Jitka Fucikova[1,2,*,], Michal Hensler[1,*], Lenka Kasikova[1], Tereza Lanickova[1,2], Josef Pasulka[1], Jana Rakova[1], Jana Drozenova[3], Tessa Fredriksen[4,5,6], Marek Hraska[1], Tereza Hrnciarova[1], Klara Sochorova[1], Daniela Rozkova[1], Ludek Sojka[1,2], Pavel Dundr[7], Jan Laco[8], Tomas Brtnicky[9], Ivan Praznovec[10], Michal J. Halaska[11], Lukas Rob[11], Ales Ryska[8], An Coosemans[12], Ignace Vergote[12,13,14], David Cibula[15], Jirina Bartunkova[1,2], Jerôme Galon[4,5,6], Lorenzo Galluzzi[16,17,18] and Radek Spisek[1,2,**]**

[1]Sotio Biotech, Prague, Czech Republic; [2]Department of Immunology, Charles University, 2nd Faculty of Medicine and University Hospital Motol, Prague, Czech Republic; [3]Department of Pathology 3rd Faculty of Medicine and University Hospital Kralovske Vinohrady, Prague, Czech Republic; [4]INSERM UMRS1138, Laboratory of Integrative Cancer Immunology, Paris, France; [5]Equipe Labellisée Ligue Contre Le Cancer, Paris, France; [6]Centre De Recherche Des Cordeliers, Sorbonne Université, Université De Paris, Paris, France; [7]Department of Pathology, 1st Faculty of Medicine, Charles University and General University Hospital, Prague; [8]The Fingerland Department of Pathology, Charles University, Faculty of Medicine and University Hospital Hradec Kralove, Czech Republic; [9]Department of Gynecology and Obstetrics, 1st Faculty of Medicine, Charles University, University Hospital Bulovka, Prague, Czech Republic; [10]Department of Gynecology and Obstetrics, Charles University, Faculty of Medicine and University Hospital Hradec Kralove, Czech Republic; [11]Department of Gynecology and Obstetrics, Charles University, 3rd Faculty of Medicine and University Hospital Kralovske Vinohrady, Prague, Czech Republic; [12]Department of Oncology, Leuven Cancer Institute, Laboratory of Tumor Immunology and Immunotherapy, KU Leuven, Belgium; [13]Department of Oncology, Leuven Cancer Institute, Laboratory of Gynaecologic Oncology, KU Leuven, Belgium; [14]Department of Gynaecology and Obstetrics, Leuven Cancer Institute, UZ Leuven, Leuven, Belgium; [15]Gynecologic Oncology Center, Department of Obstetrics and Gynecology, 1st Faculty of Medicine, Charles University and General University Hospital, Prague; [16]Department of Radiation Oncology, Weill Cornell Medical College, New York, NY, USA; [17]Sandra and Edward Meyer Cancer Center, New York, NY, USA; [18]Caryl and Israel Englander Institute for Precision Medicine, New York, NY, USA.

Running title: Tumor-targeting immune responses elicited by DC-based vaccination

Keywords: cancer immunotherapy; high grade serous ovarian carcinoma; mutational profiling; intratumoral heterogeneity; RNA sequencing; tumor neoantigens.

*Contributed equally to this work

**Correspondence to Radek Spisek (spisek@sotio.com) or Jitka Fucikova (fucikova@sotio.com) Department of Immunology, Charles University, 2nd Medical school, V Uvalu 84, Prague 5, 150 00, Czech Republic; email: fucikova@sotio.com

Conflict-of-interest disclosure: IV declares consulting for: Astra Zeneca, Clovis Oncology Inc., Carrick Therapeutics, Deciphera Pharmaceuticals, Elevar Therapeutics, F. Hoggmann-La Roche Ltd, Genmab, GSK, Immunogen Inc., Jazzpharma, Mersana, Millennium Pharmaceuticals, MSD, Novocure, Octimet Oncology NV, Oncoinvent AS, Sotio a.s., Verastem Oncology, Zentalis; contracted research for: Oncoinvent AS, Genmab; research funding from: Amgen, Roche. **LG** has received consulting fees from Astra Zeneca, Boehringer Ingelheim, Inzen and the Luke Heller TECPR2 Foundation, and he is member of Scientific Advisory Committees for Boehringer Ingelheim and OmniSEQ. The other authors declare no conflicts of interest. **RS** and **JB** are minority shareholders of Sotio Biotech a.s.. **AR** declare advisory services and invited lectures for Amgen, AstraZeneca, BMS, Eli-Lilly, Janssen-Cilag, MSD, Roche.

Translational relevance:

At odds with other neoplasms, epithelial ovarian carcinoma (EOC) is virtually insensitive to immune checkpoint inhibitors (ICIs), correlating with a limited tumor mutational burden (TMB) and scarce infiltration by immune cells. Thus, strategies to induce anticancer immune responses in patients with EOC as well as approaches that support optimal (immuno)therapeutic decision making are highly awaited. Here, we demonstrate that while patients with highly infiltrated, "hot" EOCs benefit from standard-of-care chemotherapy, subjects with poorly infiltrated, "cold" EOCs may require DC-based vaccination to jumpstart clinically relevant anticancer immune responses.

Abstract

Purpose: The successful implementation of immune checkpoint inhibitors (ICIs) in the clinical management of various solid tumors has raised considerable expectations for patients with epithelial ovarian carcinoma (EOC). However, EOC is poorly responsive to ICIs due to immunological features including limited tumor mutational burden (TMB) and poor lymphocytic infiltration. An autologous dendritic cell (DC)-based vaccine (DCVAC) has recently been shown to be safe and to significantly improve progression-free survival (PFS) in a randomized Phase II clinical trial enrolling patients with EOC (SOV01, NCT02107937).

Experimental design: We harnessed sequencing, flow cytometry, multispectral immunofluorescence microscopy, immunohistochemistry to analyze (pre-treatment) tumor and (pre-treatment and post-treatment) peripheral blood samples from 82 patients enrolled in SOV01, with the aim of identifying immunological biomarkers that would improve the clinical management of patients with EOC treated with DCVAC.

Results: Although higher-than-median TMB and abundant $CD8^+$ T cell infiltration were associated with superior clinical benefits in patients with EOC receiving standard-of-care chemotherapy, the same did not hold true in women receiving DCVAC. Conversely, superior clinical responses to DCVAC were observed in patients with lower-than-median TMB and scarce $CD8^+$ T cell infiltration. Such responses were accompanied by signs of improved effector functions and tumor-specific cytotoxicity in the peripheral blood.

Conclusions: Our findings suggest that while patients with highly infiltrated, “hot” EOCs benefit from chemotherapy, women with “cold” EOCs may instead require DC-based vaccination to jumpstart clinically relevant anticancer immune responses.

Introduction

Epithelial ovarian carcinoma (EOC) is one of the leading causes of death from gynecologic malignancies, with a 5-year survival rate of 47.8% (1). The majority of women with EOC achieve complete remission after primary or interval cytoreductive surgery followed by standard-of-care (SOC) chemotherapy with a platinum-taxane doublet and bevacizumab. Homologous recombination (HR) defects are key determinants of platinum sensitivity in patients with EOC and provide rationale for maintenance therapy with poly(ADP-ribose) polymerase (PARP) inhibitors, which is associated with improved progression-free survival (PFS) (2). However, most patients with EOC ultimately relapse and succumb to their disease, calling for the development of novel therapeutic regimens in complement or substitution of current treatments.

The successful implementation of immune checkpoint inhibitors (ICIs) in the clinical management of various solid tumors has raised considerable expectations for women with EOC (3,4). However, EOC is poorly sensitive to ICIs employed as standalone immunotherapeutic agents (5,6), correlating with limited tumor mutational burden (TMB) (7,8) and poor infiltration by $CD8^+$ cytotoxic T lymphocytes (CTLs) (9,10).

Thus, novel strategies are needed to overcome the frequent lack of pre-existing immunity in patients with EOC, potentially including chemotherapies that induce immunogenic cell death (ICD) (11), adoptive T-cell transfer strategies (12,13), and/or vaccination approaches (14,15). As most immunotherapies only benefit a small percentage of patients (4), it is also imperative to discover biomarkers that prospectively identify patients with EOC potentially achieving benefits from specific immunotherapeutic regimens, in the setting of personalized cancer immunotherapy (16).

We have recently published the results of an open label, randomized Phase II clinical study (SOV01, NCT02107937) comparing the efficacy of an autologous dendritic cell (DC)-based vaccine (DCVAC) delivered in the context of (parallel or sequential) SOC carboplatin plus

paclitaxel chemotherapy *versus* SOC only in patients with EOC (17). In this setting, DCVAC was well tolerated and significantly extended the PFS of women with EOC, but only when administered after SOC chemotherapy (17). Here, we demonstrate that while a higher-than-median TMB and robust tumor infiltration by $CD8^+$ T lymphocytes were associated with improved clinical outcome in patients from SOV01 receiving SOC chemotherapy, the same did not hold true for patients receiving DCVAC. Conversely, the clinical benefits of DCVAC were more pronounced in EOC patients with lower-than-median TMB and scant $CD8^+$ T cell infiltration by $CD8^+$ T cells. Pending validation in independent studies, our findings suggest that DCVAC stands out as a promising clinical tool to jumpstart anticancer immunity in patients with immunologically "cold" EOC.

Materials and methods

Patient characteristics. From November 18, 2013 to May 18, 2015, a total of 99 patients with EOC were randomized to receive SOC chemotherapy after debulking surgery, either as a standalone adjuvant intervention (arm C, n=31), or in the context of parallel (arm A, n=34) or sequential (arm B, n=34) DCVAC administration, as part of a randomized Phase II, multicenter clinical study (SOV01, NCT02107937) (17). A concise description of the study design is provided in **Supplemental Materials and Methods** and **Supplemental Figure 1**. Two patients from arm B were excluded from the analysis since as they did not meet inclusion criteria (17). Informed written consent was obtained according to the Declaration of Helsinki, and the study was approved by appropriate Ethical Committees (201607 S14P). The primary endpoints were safety and PFS, while the secondary endpoint was overall survival (OS). Of 97 patients randomized to treatment, 82 (85%) had samples and data available for the current analysis (**Supplemental Table 1**). Clinical findings have previously been reported (17). Baseline patient characteristics were similar across treatment groups (**Supplemental Table 2**). Pathology staging was performed according to the 8th TNM classification (2017) (18), and histological types were determined according to the current WHO classification.

Immunohistochemistry. Immunohistochemistry was performed according to conventional protocols (19-21). Briefly, tumor specimens were fixed in neutral buffered 10% formalin solution and embedded in paraffin as per standard procedures. In brief, 3 µm-thick tissue sections were deparaffinized and rehydrated in a descending alcohol series (100, 96, 70, and 50%), followed by antigen retrieval with Target Retrieval Solution (Leica) in EDTA at pH 8.0 with a heated water bath (97°C, 30 min). Sections were allowed to cool down to RT for 30 min. Endogenous peroxidase was blocked with 3% H_2O_2 for 15 min. Thereafter, sections were treated with Protein Block (DAKO) for 15 min and incubated with a primary antibody specific for CD8 for 30 min, followed by revelation of enzymatic activity with EnVision™$^{+}$/HRP, Rabbit (DAKO) for 20 min

(**Supplemental Table 3**). Finally, sections were counterstained with hematoxylin (DAKO) for 15 sec. Images of whole tumor sections were acquired using a Leica Aperio AT2 scanner (Leica).

Immunofluorescence. Immunofluorescence with antibodies specific for lysosomal associated membrane protein 3 (LAMP3; best known as DC-LAMP), CD8 and CD20 (**Supplemental Table 3**) was performed according to conventional protocols (21). Briefly, 3 μm-thick formalin-fixed paraffin-embedded (FFPE) tissue sections were deparaffinized and rehydrated in a descending alcohol series (100, 96, 70, and 50%), followed by antigen retrieval with Target Retrieval Solution (Leica) in EDTA pH 8.0 with a heated water bath (97 °C, 30 min). Sections were allowed to cool down to RT for 30 min, then treated with Signal Enhancer (Thermo Fisher Scientific) for 30 min and Blocking Buffer (Thermo Fisher Scientific) for 1 h. The DC-LAMP-specific antibody was incubated overnight at 4°C, the CD8-specific antibody for 2 hours at RT, the CD20-specific antibody for 1 hour at RT. Thereafter, slides were incubated with appropriate HRP Polymer secondary antibodies for 1 hour at RT, followed by Tyramide Signal Amplification (Thermo Fisher Scientific). Finally, sections were treated with TrueBlack Lipofuscin Autofluorescence Quencher (Biotium) for 30 sec and mounted with ProLong Gold Antifade Reagent containing DAPI (Thermo Fisher Scientific) **(Supplemental Table 3**). The specificity of the staining was determined using appropriate isotype controls. Images of whole tumor sections were acquired using a Leica Aperio AT2 scanner (Leica) (**Supplemental Figure 2**).

Cell quantification. Infiltration of tumor nests by $CD8^+$ T cells, DC-$LAMP^+$ DCs, $CD20^+$ B cells was quantified in whole tumor sections by the Calopix software (Tribvn), as published previously (19). Data are reported as absolute numbers of $CD8^+$, DC-$LAMP^+$ or $CD20^+$ cells/mm^2. Quantitative assessments were performed by three independent investigators (JF, LK, TL) and independently reviewed by an expert pathologist (JL, AR).

Immunomonitoring. Blood samples for immunomonitoring were collected at enrollment, at the end of DCVAC treatment, and at follow up (6 months after treatment) (**Supplemental Figure 1**). Lymphocyte subsets including $CD45^+$ cells; $CD3^+$, $CD4^+$, and $CD8^+$ T cells; $CD16^+CD56^+$ NK cells; and $CD19^+$ B cells were assessed in fresh blood samples using CYTO-STAT tetraCHROME CD45-FITC/CD4-RD1/CD8-ECD/CD3-PC5, CYTO-STAT tetraCHROME CD45-FITC/CD56-RD1/CD19-ECD/CD3-PC5 (Beckman Coulter), and anti-HLA-DR (Beckman Coulter) reagents (**Supplemental Table 4**). Cells were quantified by flow cytometry using a FACS CANTO II analyzer (BD Bioscience) and analyzed using FlowJo (Tree Star, Inc) (**Supplementary Figures 3A, B**).

Detection of antigen-specific T cells. The frequency of T cells specific for erb-b2 receptor tyrosine kinase 2 (ERBB2, best known as HER2), MAGE family member A3 (MAGEA3) and mucin 1, cell surface associated (MUC1) was assessed by flow cytometry according to standard procedures. In brief, peripheral blood mononuclear cells (PBMCs) were cultured for 10 days together with overlapping peptides spanning the whole sequence of HER2, MAGEA3 and MUC1 (PepMix; JPT Peptide Technologies) at a final concentration of 1 mg/mL. On days 4 and 7, 20 UI/mL IL-2 (Gentaur) was added. On day 9, PBMCs were restimulated with peptide mixtures, and 5 mg/mL brefeldin A (BioLegend) was added after 4 h of incubation. Unstimulated cells were used as negative control. Moreover, PBMCs treated with CEFT pool mixture (PepMix, JPT peptide technologies) as for the aforementioned protocol were employed as a positive control. Eventually, PBMCs were co-stained with CD3-Alexa700, CD4-PerCP-Cy5.5 and CD8-eFluor450 (Thermo Fisher Scientific) conjugates plus the Aqua Blue Live/Dead cell viability dye (Life Technologies) (**Supplemental Table 4**) for 25 min. Thereafter, cells were fixed with Fixation/Permeabilization Buffer (BD Bioscience) for 30 min, further permeabilized with Permeabilization Buffer (BD Bioscience) for 10 min and incubated with IFN-γ-PE-Cy7 and GZMB-PE (BioLegend) for 30 min. Flow cytometry was performed on an LSRFortessa Analyzer (BD), and data were analyzed with

FlowJo (Tree Star, Inc). Upon exclusion of dead cells, IFN-γ expression was considered to be antigen specific if the frequency of IFN-γ-producing T cells detected in response to peptide stimulation was at least twice the frequency of IFN-γ-producing cells detected in control conditions.

nCounter NanoString gene expression profiling. A total of 100 ng of RNA isolated from FFPE tumor sections was used to analyze expression of 770 genes involved in immune responses based on the PanCancer Immune Profiling Panel (NanoString Inc.), as per manufacturer's recommendations. Briefly, RNA was hybridized with biotin-labeled capture probes and fluorescent reporter probes for 21 hours at 65°C. Following hybridization, samples were injected into a NanoString SPRINT cartridge and loaded onto the SPRINT profiler. Following image acquisition, mRNA counts were calculated from RCC files using nSolver analysis software v4.0 (NanoString Inc.)

TMB analyses. The NGS library was prepared using TruSight Oncology 500 DNA kit (Illumina) as per manufacturer's recommendations. Denaturation of NGS libraries was achieved by bead-based normalization, according to the manufacturer protocol. Final denaturation was performed according to the NextSeqSystem Denature and dilute Guide. NGS libraries were sequenced on the NextSeq 550 using NextSeq 500/550 High Output kit v2.5 (300 cycles) in pair-end mode 2x101 bp. The TMB analysis was done using the TSO500 LocallApp. Further details are provided in **Supplemental Materials and Methods**.

Isolation of RNA from PBMCs and reverse transcription. Total RNA was isolated with the RNeasy Mini Kit (Qiagen). Cell lysates in RLT buffer enriched with 1% 2-mercaptoethanol were quickly thawed and processed as per manufacturer instructions, including a DNase I digestion step. RNA concentration and purity were determined using a NanoDrop 2000c (Thermo Scientific). Purified RNA samples were stored at -80 °C until further use. cDNA for the detection of selected

96 genes associated with immune system (**Supplemental Table 5**), was synthesized from 100 ng of total RNA using the TATAA GrandScript cDNA Synthesis Kit (TATAA Biocenter).

Statistical analysis. This study was conducted as retrospective exploratory study. PFS was defined as the time from randomization to the date of the first radiological progression or death, whichever came first. OS was calculated as the time from randomization to death from any cause. Survival analyses were estimated by Cox proportional hazard regressions and the Kaplan-Meier method, where differences between the groups of patients were calculated using the log-rank test. For Log-rank tests, the prognostic value of continuous variables was assessed using median cutoff of intra-tumoral $CD8^+$ T cell density and TMB value. The Mann-Whitney test was used to compare the density of tumor-infiltrating cells among patient groups. The Wilcoxon test was used to compare the frequency of immune markers before and after therapy. The Fisher exact test was used to compare patient distribution across subgroups. The enrichGo function from ClusterProfiles was used to identify enriched GO terms based on hypergeometric distribution. *p* values were adjusted for multiple comparisons using the Benjamini-Hochberg correction. All analyses were performed with Prism 8.4.2 (GraphPad), SAS software V.9.4, and R (http://www.r-project. org/). *p* values < 0.05 were considered statistically significant.

Data Availability Statement. The data generated in this study are available upon request to the corresponding author.

Results

TMB positively correlates with anti-tumor immunity in EOC. We first set to harness the TrueSightOnco500 panel to compare mutational profile and TMB in samples from patients with EOC involved in the SOV01 study. We identified a panel of 20 somatic mutations (*TP53, BRCA1, ARID5B, BARD1, MED12, PIK3CA, SDHA, BCORL1, KRAS, SPTA1, TET1, ZFHX3, ZNF703, ARID1A, BCOR, FANCD2, GNAS, KDM5A, MDC1, SLX4*) that were recurrent in more than 5% of these patients, which were well balanced across study arms (**Figure 1A**). Along similar lines, we did not observe a significant difference in baseline TMB in patients from different study arms (**Figure 1B**). To elucidate the impact of TMB on the EOC immune contexture, we investigated the relative expression levels of 770 genes associated with immune responses using the Nanostring PanCancer Immune Profiling Panel. We identified a set of 144 genes that were significantly overrepresented in EOC samples from patients with higher-than-median TMB (TMB^{Hi}) as compared to patients with lower-than-median TMB (TMB^{Lo}) (**Figure 1C; Supplemental Table 6**). Importantly, we chose to stratify the patient cohort based on median TMB rather than using the standard cutoff of 10 somatic mutations per Mb (22), because TMB in our cohort ranged from 0 to 10 somatic mutations per Mb (median=2.2), which is in line with published data (8,23). Gene enrichment studies based on the enrichGo function from Cluster Profiler revealed a significant association between such differentially expressed genes (DEGs) and immune system activation, especially (but not limited to) positive regulation of adaptive immune response, as well as cytotoxic T cell- and natural killer (NK) cell-mediated immunity (**Supplemental Figure 4A**). To validate these findings with an independent methodology, we analyzed the relationship between TMB status and the intratumoral abundance of $CD8^+$ CTLs, DC-$LAMP^+$ mature DCs and $CD20^+$ B cells as assessed by multispectral immunofluorescence (**Figure 1D; Supplemental Figure 2**). We observed significantly higher densities of $CD8^+$ CTLs (p=0.010), mature DC-$LAMP^+$ DCs (p=0.002) and $CD20^+$ B cells (p=0.005) in tumor samples from TMB^{Hi} vs. TMB^{Lo} EOCs (**Figure 1E**). Taken

together, these findings indicate that an elevated TMB is associated with improved immune effector functions in the EOC microenvironment.

TMB negatively correlates with superior clinical benefits in EOC patients treated with DCVAC. To assess the prognostic and predictive value of the TMB in our cohort, we evaluated PFS and OS upon stratifying the patients enrolled in the SOV01 study based on median TMB (**Figure 2A**). In arm C (patients receiving SOC chemotherapy), the TMB^{Hi} status was significantly associated with improved PFS and OS (PFS: p=0.021; OS: p=0.040; **Figure 2B**). To corroborate our findings in an independent patient cohort, we retrieved TMB values for 206 patients with high grade serous ovarian carcinoma (HGSOC) from the TCGA database and stratified them based on median TMB. Also in this setting, TMB^{Hi} patients exhibited improved OS as compared with their TMB^{Lo} counterparts (p=0.013; **Supplemental Figure 4B**). These data suggest that an elevated TMB may be indicative of an ongoing immune response that favorably affects disease outcome in patients with EOC. In line with this notion, the neoplastic lesions of TMB^{Hi} patients were abundantly infiltrated by $CD8^+$ T cells (**Figure 1E; Supplemental Figure 4C**).

Conversely, TMB^{Hi} patients from arms A and B (receiving DCVAC) did not exhibit favorable PFS and OS as compared to their TMB^{Lo} counterparts (**Figure 2C; Supplemental Figure 4D**). To obtain additional insights into the predictive value of the TMB on DCVAC efficacy, we directly compared PFS and OS in patients with TMB^{Lo} tumors from all study arms. We found that DCVAC conferred an OS advantage to patients with TMB^{Lo} EOCs irrespective of whether it was administered in parallel with or sequentially to SOC chemotherapy (Arm A: p=0.020, Arm B: p=0.010; **Figures 2D,E**), as well a PFS advantage to patients with TMB^{Lo} EOCs, but only when administered after SOC chemotherapy (Arm A: p=0.165, Arm B: p=0.007; **Figures 2D,E**). Conversely, TMB^{Hi} patients treated with DCVAC failed to exhibit improved PFS and OS as compared to TMB^{Hi} patients receiving SOC chemotherapy (**Figures 2F,G**). We obtained similar results when arms A and B of the study were analyzed as a single group of patients (OS: p=0.004;

PFS: p=0.031; **Supplemental Figure 4E, F**). Univariate Cox analysis further confirmed the increased risk for death associated with an elevated TMB in EOC patients receiving DCVAC irrespective of treatment schedule (**Table 1**).

Taken together, these findings indicate that while an elevated TMB is associated with improved disease outcome in patients with EOC treated with SOC chemotherapy, a low TMB status is associated with improved disease outcome in women with EOC receiving DCVAC.

Reduced CD8$^+$ T cell infiltration in pre-treatment tumor samples correlates with improved disease outcome in EOC patients treated with DCVAC. TMB generally correlates with immune infiltration by CD8$^+$ CTLs in multiple solid tumors, including EOC (8,24). Driven by these premises and our TMB findings, we employed the Nanostring PanCancer Immune Profiling Panel to estimate the prognostic value of 770 immune genes in EOC patients enrolled in the SOV01 study. Univariate Cox analyses identified 90 genes with a positive prognostic value in patients with EOC treated with SOC chemotherapy only (**Figure 3A** and **Supplemental Table 7**), which were globally associated with T lymphocyte activation and proliferation (**Supplemental Figure 5A**). The same genes, however, did not correlate with improved disease outcome in EOC patients receiving DCVAC, as demonstrated by unsupervised hierarchical clustering and univariate Cox regression analysis (**Figure 3A; Supplemental Table 7**).

To validate these findings with an independent approach, we harnessed immunohistochemistry for quantifying tumor-infiltrating CD8$^+$ CTLs in pre-treatment tumor samples (**Figures 3B; Supplemental Figure 5B**) and assessing their impact on PFS and OS in patients from the SOV01 study. Importantly, tumor-infiltration by CD8$^+$ CTLs at baseline did not differ across study arms (**Figure 3C**). Similarly, the proportion of EOC patients with higher-than-median intratumoral CD8$^+$ CTLs (CD8^{Hi}) was similar across study arms (**Supplemental Figure 5C**). Confirming prior

findings by us and others (9,20,25), high intratumoral levels of $CD8^+$ CTLs had a positive impact on PFS and OS in patients with EOC receiving SOC chemotherapy (PFS: p=0.003; OS: p=0.002; **Figure 3D; Supplemental Figure 6A**). Consistent with this notion, patients from arm C relapsing on SOC chemotherapy had reduced intratumoral levels of $CD8^+$ T cells, DC-$LAMP^+$ DCs and $CD20^+$ B cells as compared to non-relapsing patients (**Supplemental Figure 6B**). Conversely, the intratumoral abundance of $CD8^+$ CTLs failed to affect PFS and OS in EOC patients receiving DCVAC, irrespective of treatment schedule (**Figure 3D and Supplemental Figure 6A**). Importantly, patients with $CD8^{Lo}$ EOCs receiving DCVAC had improved OS as compared to their $CD8^{Lo}$ counterparts receiving SOC chemotherapy, irrespective of treatment schedule (Arm A: p=0.005; **Figure 3E**; Arm B: OS: p=0.011; **Figure 3F**). The $CD8^{Lo}$ status was also associated with improved PFS, but only in patients receiving DCVAC after SOC chemotherapy (Arm B: PFS: p=0.023; **Figure 3F**). In line with these findings, patients from arms A and B relapsing upon DCVAC had increased intratumoral levels of $CD8^+$ T cells, DC-$LAMP^+$ DCs and $CD19^+$ B cells as compared to non-relapsing patients (**Supplemental Figure 6C**). We obtained similar results when arms A and B of the study were analyzed as a single group of patients (OS: p=0.005; PFS: p=0.020; **Supplemental Figure 6D**). On the contrary, we were unable to observe a significant difference in PFS and OS between $CD8^{Hi}$ patients treated with SOC chemotherapy vs DCVAC, irrespective of administration schedule (**Figures 3G, H**).

Altogether, these data extend our previous findings on TMB status as they demonstrate that low intratumoral density of $CD8^+$ CTLs is linked to superior disease outcome in patients with EOC treated with DCVAC.

An immunologically "cold" immune contexture correlates with improved antitumor immunity in patients treated with DCVAC. To evaluate the development of antitumor immune

responses, we compared the transcriptional profile of PBMCs from patients enrolled in SOV01 pre- and post-DCVAC administration. Specifically, we focused on 96 genes linked to various immune cell subsets and functions, including (but not limited to): T_H1 vs T_H2 polarization, B cells, T cell activity and cytotoxicity, DCs, NK-cell activity, and immunosuppression (**Supplemental Table 5**). Samples for this study were available from 20, 21 and 17 patients from arms A, B and C, respectively. In this context, we noted that the PBMCs of $CD8^{Lo}$ patients expressed increased amounts of multiple genes involved in $CD8^+$ CTL and/or NK cell effector functions such as *CD8A*, *GZMB, GNLY,* and *IL12A* after DCVAC administration (**Figures 4A,B; Supplemental Figure 7A**). The same did not hold true for the PBMCs of patients receiving SOC chemotherapy (irrespective of CD8 status) and those of $CD8^{Hi}$ patients receiving DCVAC, with the sole exception of *CD8A* (p=0.047) (**Figures 4A,B; Supplemental Figure 7A**). Moreover, the PBMCs collected from $CD8^{Lo}$ patients post-DCVAC treatment exhibited increased levels of several genes associated with immune effector functions beyond *CD8A*, *GZMB, GNLY,* and *IL12A* (i.e., *IFNG*, *KLRB1*, *KLRK1* and *PRF1*) as compared to their $CD8^{Lo}$ counterparts receiving SOC chemotherapy (**Figures 4A,B; Supplemental Figure 7A**). However, none of these genes were significantly upregulated in the PBMCs isolated from $CD8^{Hi}$ patients post-DCVAC treatment as compared their $CD8^{Hi}$ counterparts treated with SOC chemotherapy only (**Figures 4A, B; Supplemental Figure 7A**).

To confirm and extend these findings with another technological approach, we analyzed circulating biomarkers of immune responses by flow cytometry. Confirming our transcriptional findings, we detected a significant increase in $CD56^+$ NK cells in the circulation of $CD8^{Lo}$ patients upon DCVAC administration, which persisted until follow-up, irrespective of administration schedule (**Figure 4C**). A similar increase could be documented for $CD8^+$ T cells in patients from arm A, but not for total $CD3^+$ T cells, $CD4^+$ T cells and B cells (**Figure 4C, Supplementary Figure 7B**).

Altogether these findings indicate that DCVAC elicits signs of improved effector functions in the peripheral blood of EOC patients with scant tumor infiltration by $CD8^+$ T cells, but mostly fails to alter the baseline status of these biomarkers in patients with immunologically "hot" EOC.

Antigen-specific CTL activity is increased in the blood of EOC patients with immunologically "cold" tumors after DCVAC therapy. We next assessed the ability of DCVAC to induce antigen-specific CTL responses against HER2, MAGEA3 and MUC-1 in peripheral blood of 36 patients. We selected these three tumor-associated antigens (TAAs) because they are highly expressed by the EOC cell lines (OV90 and SKOV3) used for loading autologous DCs during DCVAC manufacturing (26) (**Supplemental Figure 8**). To this aim, we evaluated the ability of circulating CTLs to secrete interferon gamma (IFNG, best known as IFN-γ) upon PBMC exposure to peptide mixture spanning multiple domains of HER2, MAGEA3 and MUC-1. Neither HER2-, neither MAGEA3- nor MUC1-specific CTL responses could be detected in PBMCs from untreated healthy donors (not shown). Conversely, the PBMCs of EOC $CD8^{Lo}$ (but not $CD8^{Hi}$) patients treated with DCVAC (irrespective of treatment schedule) contained an approximately 2-fold percentage of $CD8^+$ CTLs responding to HER2 or MAGEA3 (but not MUC1) as compared to baseline (**Figures 5A,B**). As expected, SOC chemotherapy failed to increase the percentage of CTLs secreting IFN-γ in response to stimulation with TAA-derived peptides, irrespective of intratumoral $CD8^+$ CTL density. The frequency of $CD45^+CD3^+CD8^+$ T cells responding to a pool of bacterial and viral peptides also did not change over the course of treatment (**Supplemental Figures 9A,B**).

Since TAA-specific CTL responses have been previously associated with improved disease outcome in other cohorts of cancer patients (27,28), we tested the prognostic value of TAA-specific CTLs in 36 patients with EOC from the SOV01 study receiving DCVAC. We found that DCVAC-treated patients with higher-than-median circulating frequency of HER2- or MAGEA3-specific (but not MUC-1-specific) $CD8^+$ CTLs had a trend toward improved PFS (which reached statistical

significance in the case of MAGEA3) as compared with patients with lower-than-median circulating levels of TAA-specific CTLs (**Figure 5C**).

While these data need to be confirmed in a larger cohort of DCVAC-treated patients, our findings indicate that DCVAC may boost clinically relevant TAA-specific T cell responses mostly in patients with immunologically "cold" tumors, which is the patient subset that obtained most clinical benefits from DC-based vaccination in the SOV01 trial.

Discussion

The composition of the immune infiltrate of human solid tumors, its localization and functional orientation are major predictors of patient survival and response to immunotherapeutic interventions (4,16,24,29). As compared to other solid malignancies, EOC has a reduced TMB (8,23), generally correlating with limited tumor infiltration by $CD8^+$ CTLs (30) and hence resistance to CTL-reactivating maneuvers, such as ICIs (25,31). Thus, strategies to induce anticancer immune responses in patients with EOC as well as biomarkers that improve decision making with respect to (immuno)therapeutic approach in women with EOC are highly awaited. In this context, DC-based vaccines including DCVAC (15,17) stand out as promising tools to reconfigure the immunological microenvironment of EOC in support of clinical benefit and/or improved sensitivity to ICIs (14). In line with this notion, we have recently reported the results of a randomized, Phase II clinical trial (SOV01, NCT02107937) demonstrating that DCVAC is well tolerated and significantly extends PFS over SOC chemotherapy in patients with EOC, but only when administered after (rather than in parallel to) SOC chemotherapy (17).

Here, we demonstrate that, contrarily to EOC patients receiving SOC chemotherapy (25), women with EOC obtain clinical benefits from DCVAC that manifest with circulating biomarkers of ongoing anticancer immunity when their malignancies have a low TMB and are scarcely infiltrated by $CD8^+$ CTLs, irrespective of treatment schedule. Several scenarios can be invoked to explain these apparently counterintuitive findings. For instance, the TME of patients with TMB^{Hi} EOC and robust tumor infiltration by $CD8^+$ CTLs may exhibit the activation of compensatory immunosuppressive mechanisms that keep effector immune functions at bay, not only preventing potential DCVAC-elicited CTLs from mediating anticancer effects, but also limiting the ability of DCVAC to elicit TAA-specific CTLs (25,32). This has previously been reported in patients with various solid carcinomas, including ovarian carcinoma, in which the intratumoral density of $CD8^+$ CTLs correlates with the abundance of immunosuppressive cell populations such as

$CD4^+CD25^+FOXP3^+$ regulatory T (T_{REG}) cells (33-35). Conversely, EOCs with low TMB and scant infiltration by $CD8^+$ CTLs may be relatively naïve with respect to immune infiltration at large, and hence allow (at least initially or to some degree) for the effector functions of DCVAC-driven CTLs. In further support of this interpretation, the transcriptional profile of EOC samples from the TCGA database that contain higher-than-median levels of *CD8* is enriched for a variety of transcripts expressed by immunosuppressive cells, such as V-set immunoregulatory receptor (*C10orf54*; best known as VSIR), *CD68*, *CD274* (best known as PDL1), cytotoxic T-lymphocyte associated protein 4 (*CTLA4*), ectonucleoside triphosphate diphosphohydrolase 1 (*ENTPD1*; best known as CD39), forkhead box P3 (*FOXP3*), hepatitis A virus cellular receptor 2 (*HAVCR2*; best known as TIM3), indoleamine 2, 3-dioxygenase 1 (*IDO1*), interleukin 10 (*IL-10*), lymphocyte activating 3 (*LAG3*), 5′-nucleotidase ecto (*NT5E*; best known as CD73), programmed cell death 1 (*PDCD1*; best known as PD-1), transforming growth factor beta 1 (*TGFB1*), T cell immunoreceptor with Ig and ITIM domains (*TIGIT*) and triggering receptor expressed on myeloid cells 2 (*TREM2*) (**Supplementary Figure 10**). Moreover, both a high TMB and robust infiltration by $CD8^+$ CTLs are expected to correlate with increased intratumoral heterogeneity (ITH), which confers the entire malignant lesion as an ecosystem with increased probability to escape TAA-specific CTLs by virtue of the CTL-dependent selection of TAA-negative cancer cells (36). On the contrary, a limited TMB is generally associated with reduced ITH and hence (at least theoretically) poor adaptability in response to TAA-targeting anticancer immunity. Finally, the cellular biology of TMB^{Hi} EOCs may differ considerably from that of their TMB^{Lo} counterparts so to render them resistant to DCVAC-driven CTLs, for instance as a function of altered proliferation (37,38). All these possibilities remain to be experimentally verified in the context of EOC.

Our study has various limitations. First, it is an explorative retrospective study on a relatively low number of patients with no pre-planned statistical analysis, which altogether limits statistical power. Second, the collection of post-treatment tumor biopsies was not included in the clinical trial design,

which prevents us from investigating alterations in the EOC microenvironment elicited by DCVAC. Third, blood samples collected in the course of treatment were more frequently available for patients experiencing limited side effects and overall performing well (who accepted to remain in the study until completion), as compared to patients suffering from treatment-related toxicity or progressing rapidly.

Irrespective of these and other caveats, our findings bring up two important considerations. First, they suggest that baseline TMB and T-cell infiltration may perhaps be further evaluated as a tool to guide therapeutic decisions in patients with EOC. Specifically, they suggest that while patients with TMB^{Hi} EOC and robust tumor infiltration by $CD8^+$ CTLs may benefit from SOC chemotherapy alone (and perhaps even ICIs, based on sporadic literature reports) (39,40), women with TMB^{Lo} lesions and scant tumor infiltration by $CD8^+$ CTLs may instead benefit from strategies that jumpstart anticancer immunity, such as DCVAC or radiotherapy (RT) (41). In this context, diagnostic test quantifying tumor infiltration by $CD8^+$ CTLs and approved for clinical use in other oncological indications, such as the Immunoscore, could be considered as a tool to guide patient selection and inclusion in future clinical trials (29). Second, our data lend additional support to the key importance of administration for the development of combinatorial anticancer regimens (42,43). In particular, they add to a growing preclinical literature indicating that measures that initiate anticancer immunity such as DCVAC or RT should be administered prior to (and not after or concomitant to) ICIs or other therapeutic agents that engage the effector phase of the immune response (*e.g.*, CDK4/6 inhibitors) (44,45). From this perspective, it is tempting to speculate that DCVAC followed by SOC chemotherapy and/or ICI-based immunotherapy may mediate even more pronounced anticancer effects than the DCVAC-based regimens tested in SOV01, based on the rationale that (1) DCVAC would initially promote at least some degree of tumor reactivity by $CD8^+$ CTLs (as documented in this study by an increased in circulating TAA-specific $CD8^+$ CTLs), (2) SOC chemotherapy is more active in patients with "hot" EOCs (as demonstrated in this study and

various others) (46,47), and (3) that patients with non-EOC tumors responding to ICIs generally exhibit elevated tumor infiltration by T cells at baseline (48-50). Additional clinical trials are needed to address these possibilities as well as the potential value of TMB and $CD8^+$ CTL infiltration at baseline as biomarkers to guide decision making in the clinical management of EOC.

Acknowledgements: This study was sponsored by Sotio Biotech, Prague. **JL** and **AR** were supported by the project BBMRI-CZ LM2018125, by the program PROGRES Q40/11, and by the Cooperatio Program, research area DIAG. **LG** is supported by a Breakthrough Level 2 grant from the US Department of Defense (DoD), Breast Cancer Research Program (BRCP) (#BC180476P1), by the 2019 Laura Ziskin Prize in Translational Research (#ZP-6177, PI: Formenti) from the Stand Up to Cancer (SU2C), by a Mantle Cell Lymphoma Research Initiative (MCL-RI, PI: Chen-Kiang) grant from the Leukemia and Lymphoma Society (LLS), by a startup grant from the Dept. of Radiation Oncology at Weill Cornell Medicine (New York, US), by a Rapid Response Grant from the Functional Genomics Initiative (New York, US), by industrial collaborations with Lytix (Oslo, Norway) and Phosplatin (New York, US), and by donations from Phosplatin (New York, US), the Luke Heller TECPR2 Foundation (Boston, US), Onxeo (Paris, France) and Sotio Biotech a.s. (Prague, Czech Republic). **LR** and **MHa** were supported by Cooperatio program, Maternal and Childhood Care 207035, 3rd Medical Faculty, Charles University. **PD** was supported by Ministry of Health, CZ, research project RVO 64165.

Contributions: Concept and design: JF, MH, MH, TH, JB; development of methodology: JF, MH, LK, acquisition of data: JF, MH, LK, TL, JR, JD, TF, MH, TH, KS, DR, LS, PD, TB, IP, MHa, LR, AR, DC, ; analysis and interpretation of data: JF, MH, LK, TF, JP, MHa, TH, AC, IV, DC, JG, JG ; writing, review, and/or revision of the manuscript: JF, MH, LK, MH, TH, JB, JG, LR, RS; study supervision: JF, MH, JB, LG, RS

References

1. Bray F, Ferlay J, Soerjomataram I, Siegel RL, Torre LA, Jemal A. Global cancer statistics 2018: GLOBOCAN estimates of incidence and mortality worldwide for 36 cancers in 185 countries. CA Cancer J Clin **2018**;68(6):394-424 doi 10.3322/caac.21492.

2. Gonzalez-Martin A, Pothuri B, Vergote I, DePont Christensen R, Graybill W, Mirza MR, *et al.* Niraparib in Patients with Newly Diagnosed Advanced Ovarian Cancer. N Engl J Med **2019**;381(25):2391-402 doi 10.1056/NEJMoa1910962.

3. Sharma P, Allison JP. Immune checkpoint targeting in cancer therapy: toward combination strategies with curative potential. Cell **2015**;161(2):205-14 doi 10.1016/j.cell.2015.03.030.

4. Galluzzi L, Chan TA, Kroemer G, Wolchok JD, Lopez-Soto A. The hallmarks of successful anticancer immunotherapy. Sci Transl Med **2018**;10(459) doi 10.1126/scitranslmed.aat7807.

5. Monk BJ, Colombo N, Oza AM, Fujiwara K, Birrer MJ, Randall L, *et al.* Chemotherapy with or without avelumab followed by avelumab maintenance versus chemotherapy alone in patients with previously untreated epithelial ovarian cancer (JAVELIN Ovarian 100): an open-label, randomised, phase 3 trial. Lancet Oncol **2021**;22(9):1275-89 doi 10.1016/S1470-2045(21)00342-9.

6. Moore KN, Bookman M, Sehouli J, Miller A, Anderson C, Scambia G, *et al.* Atezolizumab, Bevacizumab, and Chemotherapy for Newly Diagnosed Stage III or IV Ovarian Cancer: Placebo-Controlled Randomized Phase III Trial (IMagyn050/GOG 3015/ENGOT-OV39). J Clin Oncol **2021**:JCO2100306 doi 10.1200/JCO.21.00306.

7. Chan TA, Yarchoan M, Jaffee E, Swanton C, Quezada SA, Stenzinger A, *et al.* Development of tumor mutation burden as an immunotherapy biomarker: utility for the oncology clinic. Ann Oncol **2019**;30(1):44-56 doi 10.1093/annonc/mdy495.

8. Sha D, Jin Z, Budczies J, Kluck K, Stenzinger A, Sinicrope FA. Tumor Mutational Burden as a Predictive Biomarker in Solid Tumors. Cancer Discov **2020**;10(12):1808-25 doi 10.1158/2159-8290.CD-20-0522.

9. Zhang L, Conejo-Garcia JR, Katsaros D, Gimotty PA, Massobrio M, Regnani G, *et al.* Intratumoral T cells, recurrence, and survival in epithelial ovarian cancer. N Engl J Med **2003**;348(3):203-13 doi 10.1056/NEJMoa020177.

10. Hwang WT, Adams SF, Tahirovic E, Hagemann IS, Coukos G. Prognostic significance of tumor-infiltrating T cells in ovarian cancer: a meta-analysis. Gynecol Oncol **2012**;124(2):192-8 doi 10.1016/j.ygyno.2011.09.039.

11. Galluzzi L, Vitale I, Warren S, Adjemian S, Agostinis P, Martinez AB, *et al.* Consensus guidelines for the definition, detection and interpretation of immunogenic cell death. J Immunother Cancer **2020**;8(1) doi 10.1136/jitc-2019-000337.

12. Van der Meer JMR, de Jonge P, van der Waart AB, Geerlings AC, Moonen JP, Brummelman J, *et al.* CD34(+) progenitor-derived NK cell and gemcitabine combination therapy increases killing of ovarian cancer cells in NOD/SCID/IL2Rg(null) mice. Oncoimmunology **2021**;10(1):1981049 doi 10.1080/2162402X.2021.1981049.

13. Pedersen M, Westergaard MCW, Milne K, Nielsen M, Borch TH, Poulsen LG, *et al.* Adoptive cell therapy with tumor-infiltrating lymphocytes in patients with metastatic ovarian cancer: a pilot study. Oncoimmunology **2018**;7(12):e1502905 doi 10.1080/2162402X.2018.1502905.

14. Wculek SK, Cueto FJ, Mujal AM, Melero I, Krummel MF, Sancho D. Dendritic cells in cancer immunology and immunotherapy. Nat Rev Immunol **2020**;20(1):7-24 doi 10.1038/s41577-019-0210-z.

15. Cibula D, Rob L, Mallmann P, Knapp P, Klat J, Chovanec J, *et al.* Dendritic cell-based immunotherapy (DCVAC/OvCa) combined with second-line chemotherapy in platinum-sensitive ovarian cancer (SOV02): A randomized, open-label, phase 2 trial. Gynecol Oncol **2021** doi 10.1016/j.ygyno.2021.07.003.

16. Galon J, Bruni D. Approaches to treat immune hot, altered and cold tumours with combination immunotherapies. Nat Rev Drug Discov **2019**;18(3):197-218 doi 10.1038/s41573-018-0007-y.

17. Rob L, Cibula D, Knapp P, Mallmann P, Klat J, Minar L, *et al.* Safety and efficacy of dendritic cell-based immunotherapy DCVAC/OvCa added to first-line chemotherapy (carboplatin plus paclitaxel) for epithelial ovarian cancer: a phase 2, open-label, multicenter, randomized trial. J Immunother Cancer **2022**;10(1) doi 10.1136/jitc-2021-003190.

18. O'Sullivan B, Brierley J, Byrd D, Bosman F, Kehoe S, Kossary C, *et al.* The TNM classification of malignant tumours-towards common understanding and reasonable expectations. Lancet Oncol **2017**;18(7):849-51 doi 10.1016/S1470-2045(17)30438-2.

19. Goc J, Germain C, Vo-Bourgais TK, Lupo A, Klein C, Knockaert S, *et al.* Dendritic cells in tumor-associated tertiary lymphoid structures signal a Th1 cytotoxic immune contexture and license the positive prognostic value of infiltrating CD8+ T cells. Cancer Res **2014**;74(3):705-15 doi 10.1158/0008-5472.CAN-13-1342.

20. Truxova I, Kasikova L, Hensler M, Skapa P, Laco J, Pecen L, *et al.* Mature dendritic cells correlate with favorable immune infiltrate and improved prognosis in ovarian carcinoma patients. J Immunother Cancer **2018**;6(1):139 doi 10.1186/s40425-018-0446-3.

21. Fucikova J, Rakova J, Hensler M, Kasikova L, Belicova L, Hladikova K, *et al.* TIM-3 Dictates Functional Orientation of the Immune Infiltrate in Ovarian Cancer. Clin Cancer Res **2019**;25(15):4820-31 doi 10.1158/1078-0432.CCR-18-4175.

22. McGrail DJ, Pilie PG, Rashid NU, Voorwerk L, Slagter M, Kok M, *et al.* High tumor mutation burden fails to predict immune checkpoint blockade response across all cancer types. Ann Oncol **2021**;32(5):661-72 doi 10.1016/j.annonc.2021.02.006.

23. Alexandrov LB, Nik-Zainal S, Wedge DC, Aparicio SA, Behjati S, Biankin AV, *et al.* Signatures of mutational processes in human cancer. Nature **2013**;500(7463):415-21 doi 10.1038/nature12477.

24. Fridman WH, Zitvogel L, Sautes-Fridman C, Kroemer G. The immune contexture in cancer prognosis and treatment. Nat Rev Clin Oncol **2017**;14(12):717-34 doi 10.1038/nrclinonc.2017.101.

25. Fucikova J, Coosemans A, Orsulic S, Cibula D, Vergote I, Galluzzi L, *et al.* Immunological configuration of ovarian carcinoma: features and impact on disease outcome. J Immunother Cancer **2021**;9(10) doi 10.1136/jitc-2021-002873.

26. Kloudova K, Hromadkova H, Partlova S, Brtnicky T, Rob L, Bartunkova J, *et al.* Expression of tumor antigens on primary ovarian cancer cells compared to established ovarian cancer cell lines. Oncotarget **2016**;7(29):46120-6 doi 10.18632/oncotarget.10028.

27. Antonarakis ES, Small EJ, Petrylak DP, Quinn DI, Kibel AS, Chang NN, *et al.* Antigen-Specific CD8 Lytic Phenotype Induced by Sipuleucel-T in Hormone-Sensitive or Castration-

Resistant Prostate Cancer and Association with Overall Survival. Clin Cancer Res **2018**;24(19):4662-71 doi 10.1158/1078-0432.CCR-18-0638.

28. Maby P, Galon J, Latouche JB. Frameshift mutations, neoantigens and tumor-specific CD8(+) T cells in microsatellite unstable colorectal cancers. Oncoimmunology **2016**;5(5):e1115943 doi 10.1080/2162402X.2015.1115943.

29. Bruni D, Angell HK, Galon J. The immune contexture and Immunoscore in cancer prognosis and therapeutic efficacy. Nat Rev Cancer **2020**;20(11):662-80 doi 10.1038/s41568-020-0285-7.

30. Fan S, Gao X, Qin Q, Li H, Yuan Z, Zhao S. Association between tumor mutation burden and immune infiltration in ovarian cancer. Int Immunopharmacol **2020**;89(Pt A):107126 doi 10.1016/j.intimp.2020.107126.

31. Duraiswamy J, Freeman GJ, Coukos G. Therapeutic PD-1 pathway blockade augments with other modalities of immunotherapy T-cell function to prevent immune decline in ovarian cancer. Cancer Res **2013**;73(23):6900-12 doi 10.1158/0008-5472.CAN-13-1550.

32. Lucca LE, Dominguez-Villar M. Modulation of regulatory T cell function and stability by co-inhibitory receptors. Nat Rev Immunol **2020**;20(11):680-93 doi 10.1038/s41577-020-0296-3.

33. Milne K, Kobel M, Kalloger SE, Barnes RO, Gao D, Gilks CB*, et al.* Systematic analysis of immune infiltrates in high-grade serous ovarian cancer reveals CD20, FoxP3 and TIA-1 as positive prognostic factors. PLoS One **2009**;4(7):e6412 doi 10.1371/journal.pone.0006412.

34. Derks S, de Klerk LK, Xu X, Fleitas T, Liu KX, Liu Y*, et al.* Characterizing diversity in the tumor-immune microenvironment of distinct subclasses of gastroesophageal adenocarcinomas. Ann Oncol **2020**;31(8):1011-20 doi 10.1016/j.annonc.2020.04.011.

35. Petitprez F, de Reynies A, Keung EZ, Chen TW, Sun CM, Calderaro J*, et al.* B cells are associated with survival and immunotherapy response in sarcoma. Nature **2020**;577(7791):556-60 doi 10.1038/s41586-019-1906-8.

36. Vitale I, Shema E, Loi S, Galluzzi L. Intratumoral heterogeneity in cancer progression and response to immunotherapy. Nat Med **2021**;27(2):212-24 doi 10.1038/s41591-021-01233-9.

37. Pabla S, Conroy JM, Nesline MK, Glenn ST, Papanicolau-Sengos A, Burgher B*, et al.* Proliferative potential and resistance to immune checkpoint blockade in lung cancer patients. J Immunother Cancer **2019**;7(1):27 doi 10.1186/s40425-019-0506-3.

38. Zhang T, Pabla S, Lenzo FL, Conroy JM, Nesline MK, Glenn ST*, et al.* Proliferative potential and response to nivolumab in clear cell renal cell carcinoma patients. Oncoimmunology **2020**;9(1):1773200 doi 10.1080/2162402X.2020.1773200.

39. Liu JF, Gordon M, Veneris J, Braiteh F, Balmanoukian A, Eder JP*, et al.* Safety, clinical activity and biomarker assessments of atezolizumab from a Phase I study in advanced/recurrent ovarian and uterine cancers. Gynecol Oncol **2019**;154(2):314-22 doi 10.1016/j.ygyno.2019.05.021.

40. Mehnert JM, Panda A, Zhong H, Hirshfield K, Damare S, Lane K*, et al.* Immune activation and response to pembrolizumab in POLE-mutant endometrial cancer. J Clin Invest **2016**;126(6):2334-40 doi 10.1172/JCI84940.

41. Rodriguez-Ruiz ME, Vitale I, Harrington KJ, Melero I, Galluzzi L. Immunological impact of cell death signaling driven by radiation on the tumor microenvironment. Nat Immunol **2020**;21(2):120-34 doi 10.1038/s41590-019-0561-4.

42. Petroni G, Galluzzi L. Impact of treatment schedule on the efficacy of cytostatic and immunostimulatory agents. Oncoimmunology **2021**;10(1):1889101 doi 10.1080/2162402X.2021.1889101.

43. Coosemans A, Vankerckhoven A, Baert T, Boon L, Ruts H, Riva M*, et al.* Combining conventional therapy with immunotherapy: A risky business? Eur J Cancer **2019**;113:41-4 doi 10.1016/j.ejca.2019.02.014.

44. Petroni G, Buque A, Yamazaki T, Bloy N, Liberto MD, Chen-Kiang S*, et al.* Radiotherapy Delivered before CDK4/6 Inhibitors Mediates Superior Therapeutic Effects in ER(+) Breast Cancer. Clin Cancer Res **2021**;27(7):1855-63 doi 10.1158/1078-0432.CCR-20-3871.

45. Petroni G, Cantley LC, Santambrogio L, Formenti SC, Galluzzi L. Radiotherapy as a tool to elicit clinically actionable signalling pathways in cancer. Nat Rev Clin Oncol **2022**;19(2):114-31 doi 10.1038/s41571-021-00579-w.

46. Webb JR, Milne K, Watson P, Deleeuw RJ, Nelson BH. Tumor-infiltrating lymphocytes expressing the tissue resident memory marker CD103 are associated with increased survival in

high-grade serous ovarian cancer. Clin Cancer Res **2014**;20(2):434-44 doi 10.1158/1078-0432.CCR-13-1877.

47. Leffers N, Gooden MJ, de Jong RA, Hoogeboom BN, ten Hoor KA, Hollema H*, et al.* Prognostic significance of tumor-infiltrating T-lymphocytes in primary and metastatic lesions of advanced stage ovarian cancer. Cancer Immunol Immunother **2009**;58(3):449-59 doi 10.1007/s00262-008-0583-5.

48. Tumeh PC, Harview CL, Yearley JH, Shintaku IP, Taylor EJ, Robert L*, et al.* PD-1 blockade induces responses by inhibiting adaptive immune resistance. Nature **2014**;515(7528):568-71 doi 10.1038/nature13954.

49. Van Allen EM, Miao D, Schilling B, Shukla SA, Blank C, Zimmer L*, et al.* Genomic correlates of response to CTLA-4 blockade in metastatic melanoma. Science **2015**;350(6257):207-11 doi 10.1126/science.aad0095.

50. Huang AC, Postow MA, Orlowski RJ, Mick R, Bengsch B, Manne S*, et al.* T-cell invigoration to tumour burden ratio associated with anti-PD-1 response. Nature **2017**;545(7652):60-5 doi 10.1038/nature22079.

Table 1. Univariate Cox proportional hazard analyses

Overall survival Arm A			Overall survival Arm B			Overall survival Arm C		
Variable	**HR (95% CI)**	***p***	**Variable**	**HR (95% CI)**	***p***	**Variable**	**HR (95% CI)**	***p***
TMB	1.38 (1.04-1.84)	**0.027**	TMB	1.72 (1.01-2.93)	**0.046**	TMB	0.77 (0.56-1)	0.064
$CD8^+$ T cells	1 (1.00-1.01)	0.100	$CD8^+$ T cells	1 (0.99-1)	0.5	$CD8^+$ T cells	0.99 (0.98-1)	0.045

Legends to Main Display Items

***Figure 1*. Tumor mutational burden positively correlate with anti-tumor immunity in ovarian carcinoma**

(A) Oncoplot showing the profile of somatic mutations in 82 tumors annotated by study arm and clinical outcome.

(B) Violin plot showing the somatic mutations prevalence (mutations per megabase) in individual study arms. Statistical significance was calculated by the Mann–Whitney test.

(C) Hierarchical clustering of 144 genes that were significantly overrepresented in TMB^{Hi} *versus* TMB^{Lo} samples (no=82) from study, as determined by PanCancer Immune Profiling Panel from NanoString.

(D) Representative images of CD8, CD20, and DC-LAMP multispectral immunofluorescence (left). Cells expressing CD8 (purple arrow), CD20 (yellow arrow), and DC-LAMP (green arrow). For automated counting, Calopix software allows cell segmentation based on DAPI staining of the nucleus and morphometric characteristics (right). Scale bar, 25μm

(E) Density of $CD8^+$, $CD20^+$ and DC-$LAMP^+$ cells in TMB^{Hi} and TMB^{Lo} samples (no=82), as determined by immunostaining. Statistical significance was calculated by the Mann–Whitney test. *p* values are indicated.

***Figure 2*. Low tumor mutational burden (TMB) associate with better clinical response to DCVAC therapy**

(A) Distribution of TMB in study arms, with median display. **(B)** Progression-free survival (PFS) and overall survival (OS) of 26 patients from study arm C (SOC) upon stratification based on

median value of TMB. **(C)** OS of 30 and 26 patients from study arm A and B (DCVAC), respectively, based on median stratification. **(D-G)** Direct comparison of PFS and OS upon stratifying study arm C patients (SOC) and study arm A and B patients (DCVAC), respectively, based on median value of TMB into TMB^{Lo} **(D, E)** and TMB^{Hi} **(F, G)** group. Survival curves were estimated by the Kaplan-Meier method, and differences between groups were evaluated using log-rank test. Number of patients at risk and *p* values are reported.

Figure 3. **The highest clinical benefit from DCVAC therapy was observed in patients with immunologically "cold" tumors**

(A) Hierarchical clustering heatmap of differentially expressed genes in tumor samples of patients in distinct study arms annotated by overall survival (OS) and progression-free survival (PFS), determined by Pan Cancer Immune Profiling Panel (Nanostring).

(B) Representative images of CD8 immunostaining. Scale bar, 1000, 100 and 10 μm.

(C) Violin plot showing the density of $CD8^+$ T cells/mm^2 in individual study arms. Statistical significance was calculated by the Mann–Whitney test.

(D) OS of patients randomized in individual study arms stratified based on median value of intra-tumoral $CD8^+$ T cells. **(E-H)** Direct comparison of PFS and OS upon stratifying study arm C patients (SOC) and study arm A and B patients (DCVAC), respectively, based on median value of $CD8^+$ T cells into $CD8^{Lo}$ **(E, F)** and $CD8^{Hi}$ **(G, H)** group. Survival curves were estimated by the Kaplan-Meier method, and differences between groups were evaluated using log-rank test. Number of patients at risk and *p* values are reported.

Figure 4. **Immunologically naïve immune tumor contexture correlate with improved antitumor immunity in peripheral blood of DCVAC patients**

(A) Prior and post therapy biomolecular signatures of PBMCs in $CD8^{Lo}$ patients from SOV01 all study arms.

(B) Fold change of relative expression levels of genes: *CD8A*, *GZMB, GNLY, IL12A, IFNG, KLRB1, KLRK1, PRF1* differentially expressed in peripheral blood of control and DCVAC patients based on $CD8^+$ T cells density in tumor. Statistical significance was calculated by the Wilcoxon test. *p* values are indicated. All statistically significant differences are reported.

(C) The percentage $CD4^+$ T cells, $CD8^+$ T cells and $CD56^+$ NK cells in peripheral blood of SOC $CD8^{Lo}$, SOC $CD8^{Hi}$, $DCVAC^A$ $CD8^{Lo}$, $DCVAC^A$ $CD8^{Hi}$, $DCVAC^B$ $CD8^{Lo}$ and $DCVAC^B$ $CD8^{Hi}$ patients in prior, post and follow up time. Statistical significance was calculated by the Wilcoxon test. *p* values are indicated.

Figure 5. **TAAs specific CTLs activity is increased by DCVAC treatment particularly in patients with immunologically naïve immune tumor contexture**

(A, B) Representative dot plots and the percentage of IFN-γ secreting $CD45^+CD3^+CD8^+$ T cells from SOC $CD8^{Lo}$, SOC $CD8^{Hi}$, $DCVAC^A$ $CD8^{Lo}$, $DCVAC^A$ $CD8^{Hi}$, $DCVAC^B$ $CD8^{Lo}$ and $DCVAC^B$ $CD8^{Hi}$ patients prior and post therapy, upon exposure of the corresponding PBMCs to peptide mixture spanning HER2, MAGEA3 and MUC-1. Statistical significance was calculated by the Mann-Whitney test. *p* values are indicated.

(D) Progression-free survival (PFS) of 36 DCVAC patients (arm A+B) based on median stratification of HER2, MAGEA3 and MUC-1 specific CTLs in peripheral blood of patients. Survival curves were estimated by the Kaplan-Meier method, and differences between groups were evaluated using log-rank test. Number of patients at risk and *p* values are reported.

Figure 1

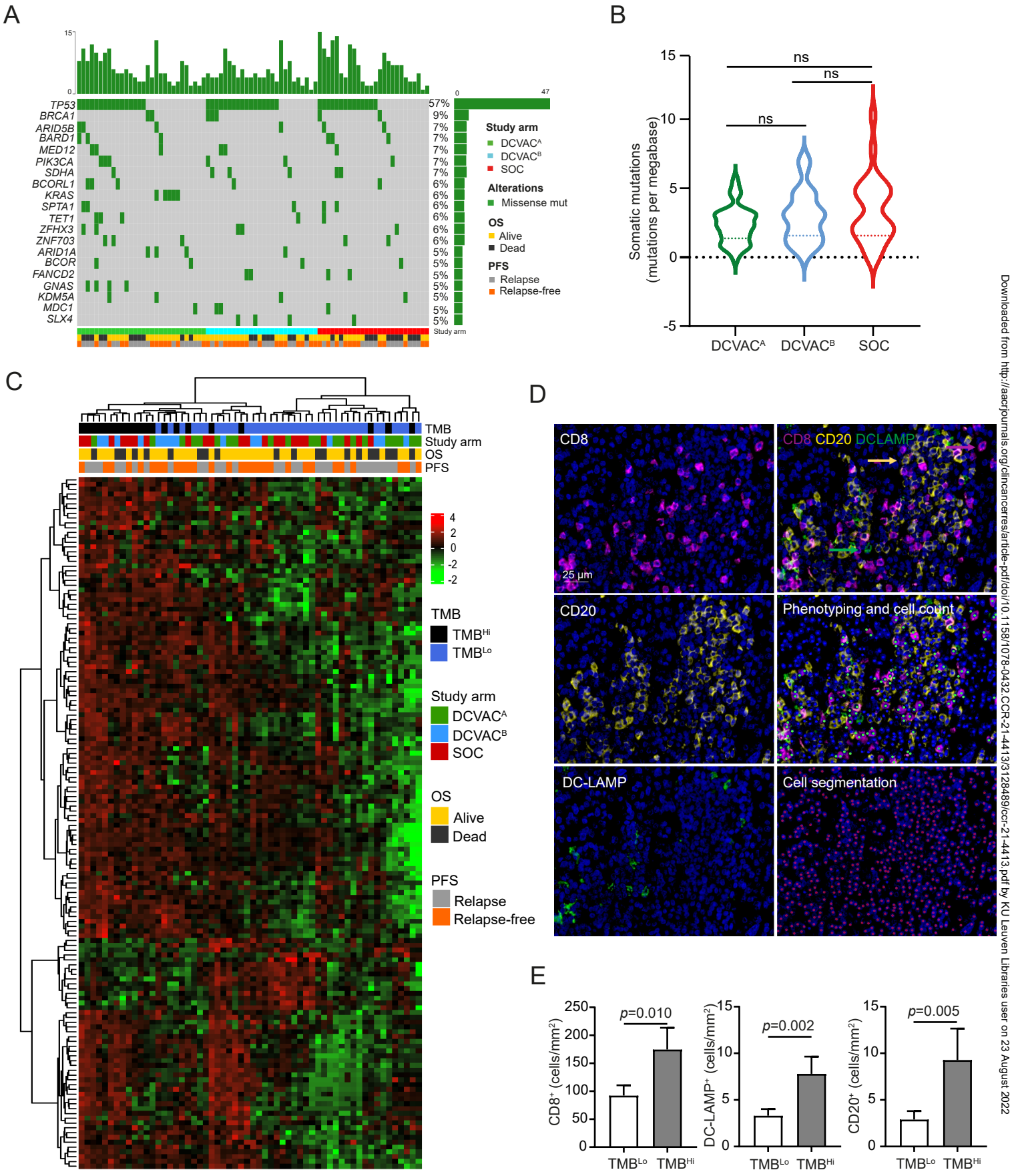

Figure 2

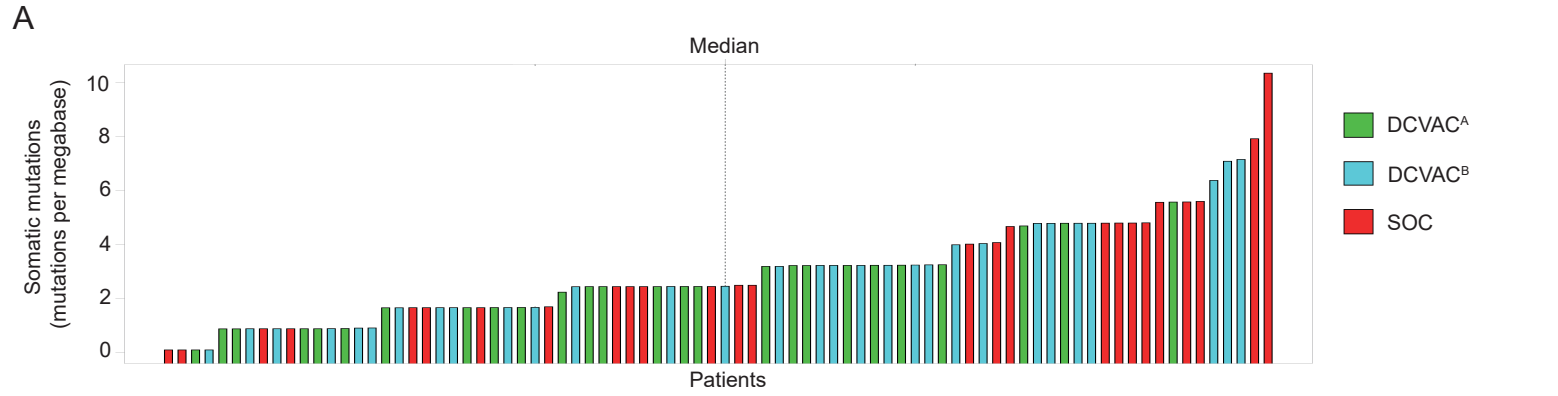

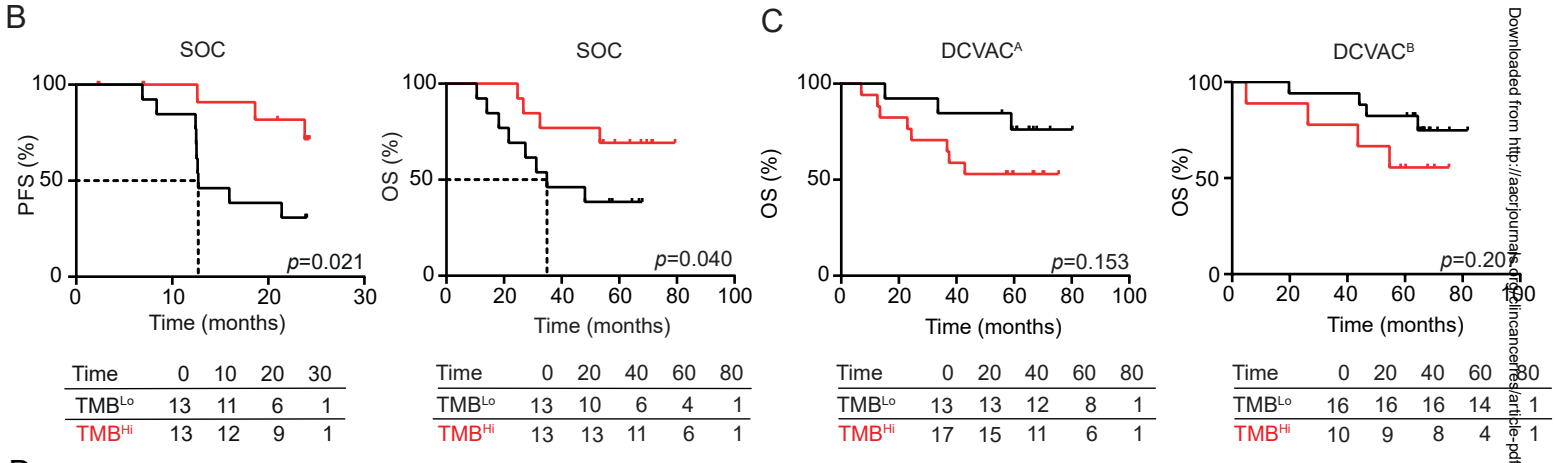

Time	0	10	20	30
TMB^Lo	13	11	6	1
TMB^Hi	13	12	9	1

Time	0	20	40	60	80
TMB^Lo	13	10	6	4	1
TMB^Hi	13	13	11	6	1

Time	0	20	40	60	80
TMB^Lo	13	13	12	8	1
TMB^Hi	17	15	11	6	1

Time	0	20	40	60	80
TMB^Lo	16	16	16	14	1
TMB^Hi	10	9	8	4	1

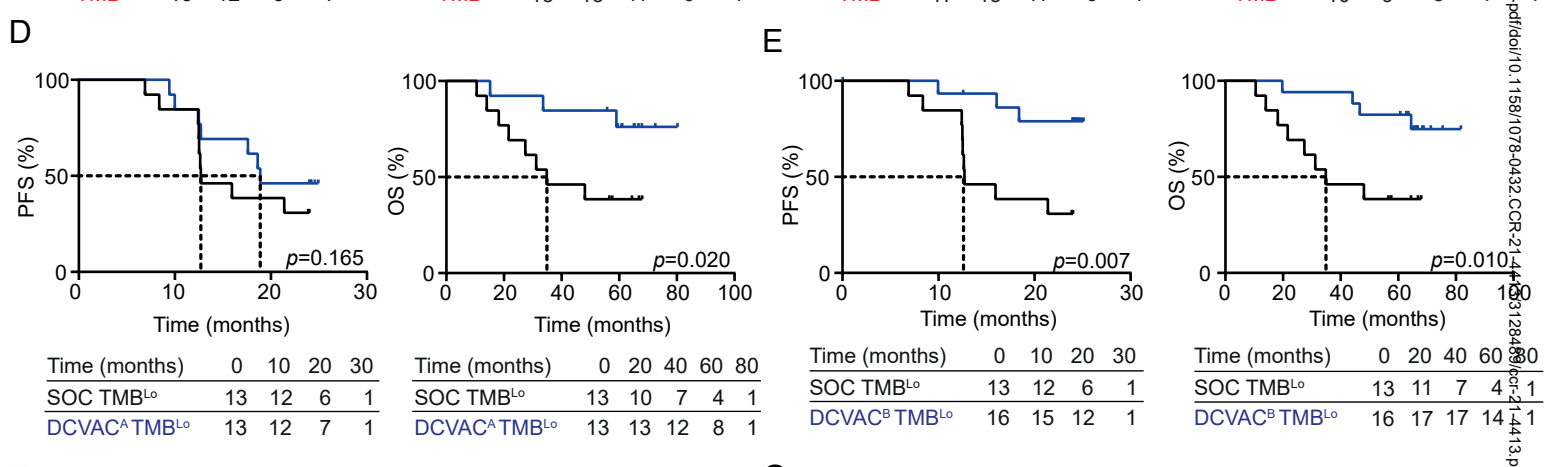

Time (months)	0	10	20	30
SOC TMB^Lo	13	12	6	1
DCVAC^A TMB^Lo	13	12	7	1

Time (months)	0	20	40	60	80
SOC TMB^Lo	13	10	7	4	1
DCVAC^A TMB^Lo	13	13	12	8	1

Time (months)	0	10	20	30
SOC TMB^Lo	13	12	6	1
DCVAC^B TMB^Lo	16	15	12	1

Time (months)	0	20	40	60	80
SOC TMB^Lo	13	11	7	4	1
DCVAC^B TMB^Lo	16	17	17	14	1

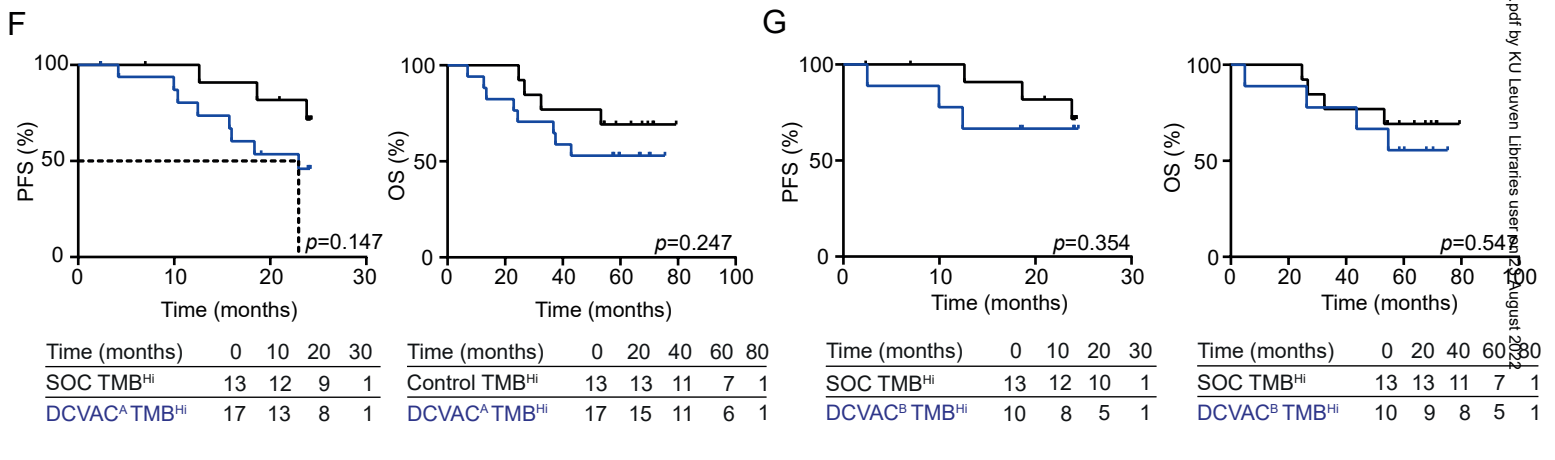

Time (months)	0	10	20	30
SOC TMB^Hi	13	12	9	1
DCVAC^A TMB^Hi	17	13	8	1

Time (months)	0	20	40	60	80
Control TMB^Hi	13	13	11	7	1
DCVAC^A TMB^Hi	17	15	11	6	1

Time (months)	0	10	20	30
SOC TMB^Hi	13	12	10	1
DCVAC^B TMB^Hi	10	8	5	1

Time (months)	0	20	40	60	80
SOC TMB^Hi	13	13	11	7	1
DCVAC^B TMB^Hi	10	9	8	5	1

Figure 3

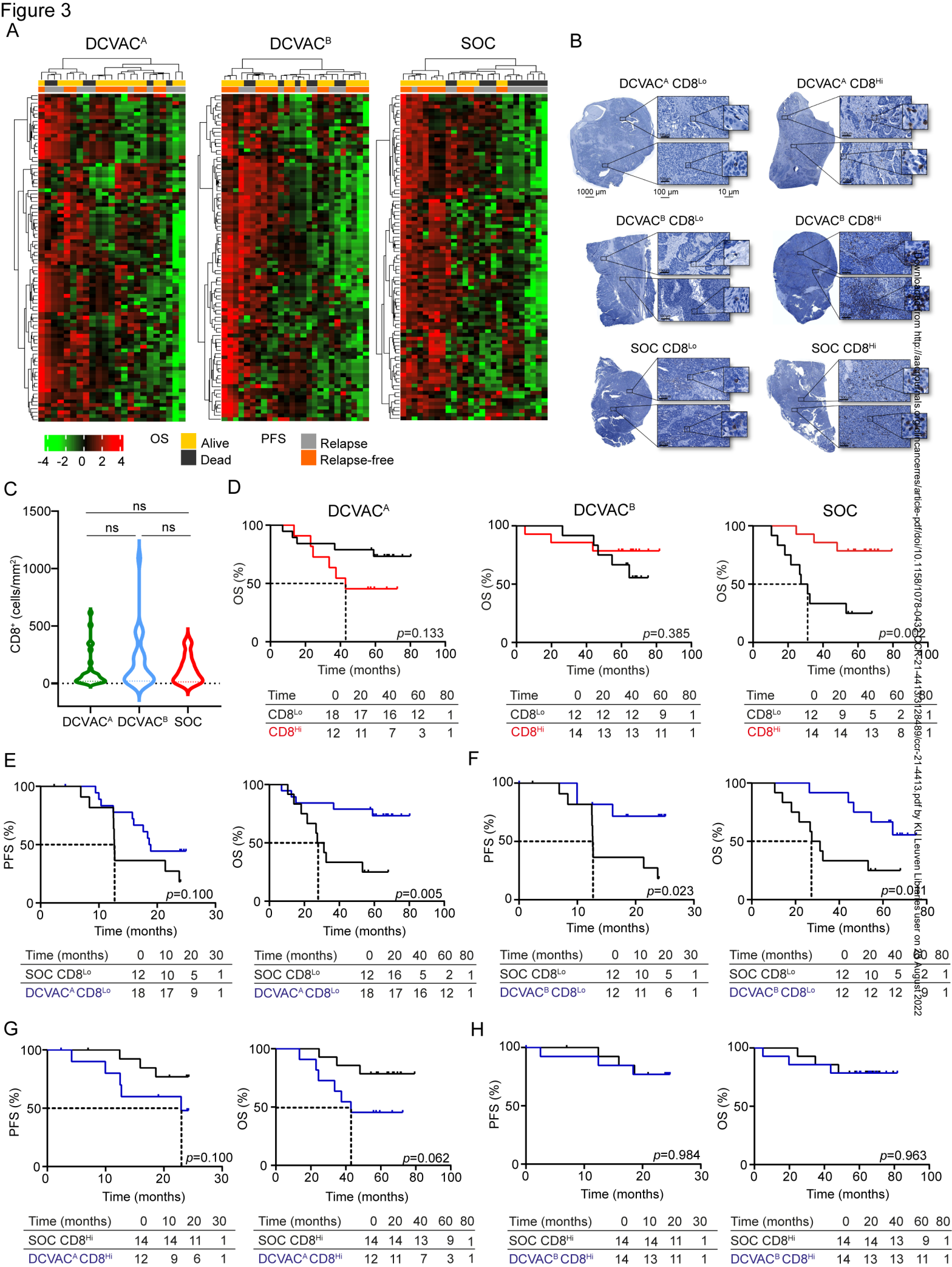

Figure 4

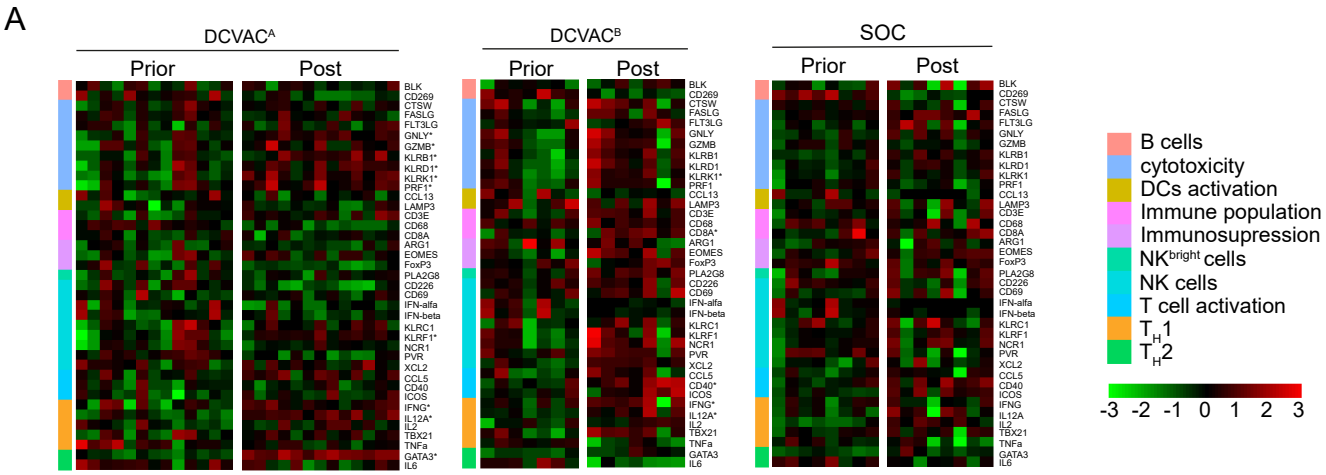

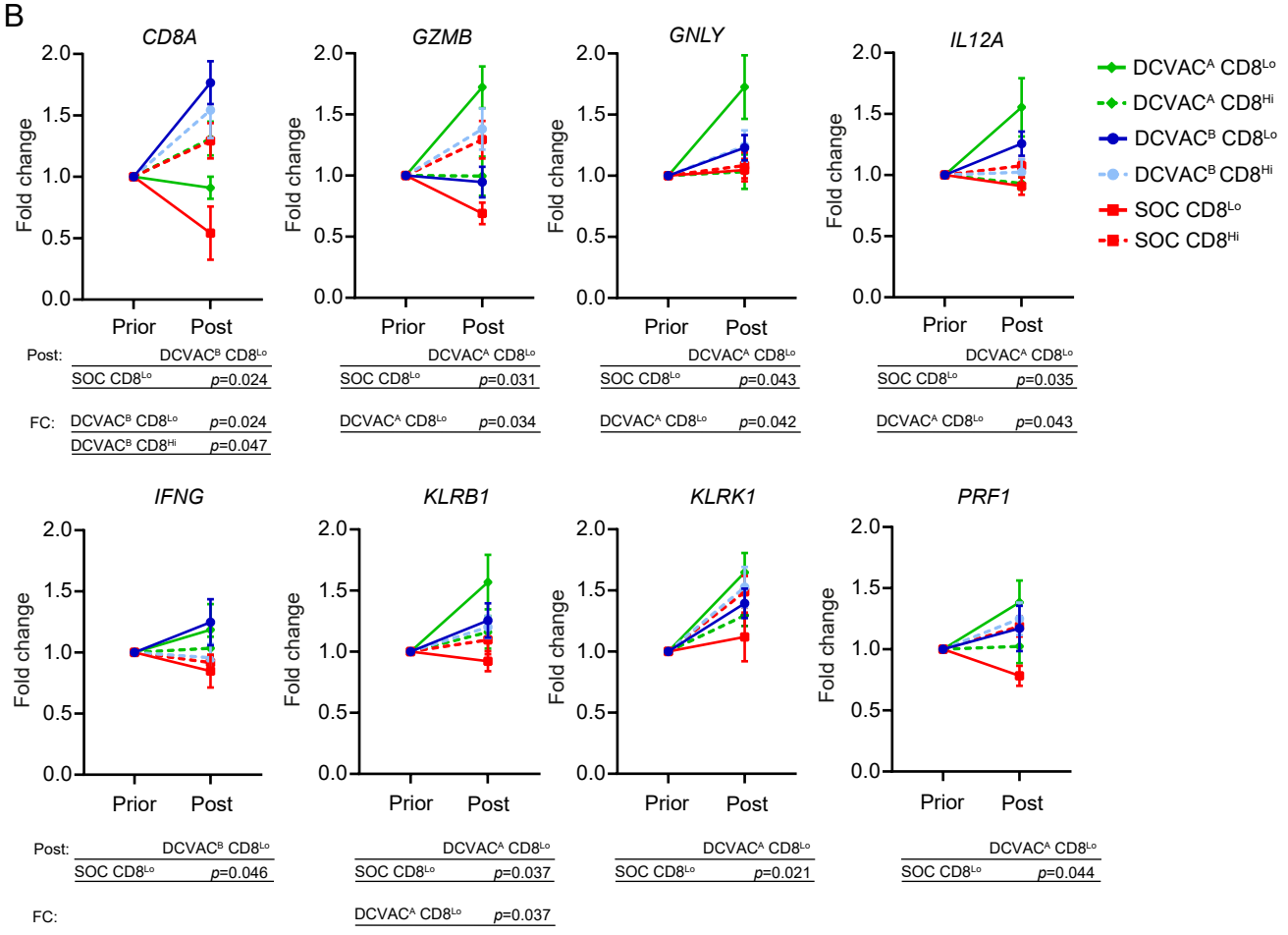

Post:	DCVAC^B CD8^Lo		
	SOC CD8^Lo	p=0.024	
FC:	DCVAC^B CD8^Lo	p=0.024	
	DCVAC^B CD8^Hi	p=0.047	

Post:	DCVAC^A CD8^Lo	
	SOC CD8^Lo	p=0.031
FC:	DCVAC^A CD8^Lo	p=0.034

Post:	DCVAC^A CD8^Lo	
	SOC CD8^Lo	p=0.043
FC:	DCVAC^A CD8^Lo	p=0.042

Post:	DCVAC^A CD8^Lo	
	SOC CD8^Lo	p=0.035
FC:	DCVAC^A CD8^Lo	p=0.043

Post:	DCVAC^B CD8^Lo	
	SOC CD8^Lo	p=0.046
FC:		

Post:	DCVAC^A CD8^Lo	
	SOC CD8^Lo	p=0.037
FC:	DCVAC^A CD8^Lo	p=0.037

Post:	DCVAC^A CD8^Lo	
	SOC CD8^Lo	p=0.021
FC:		

Post:	DCVAC^A CD8^Lo	
	SOC CD8^Lo	p=0.044
FC:		

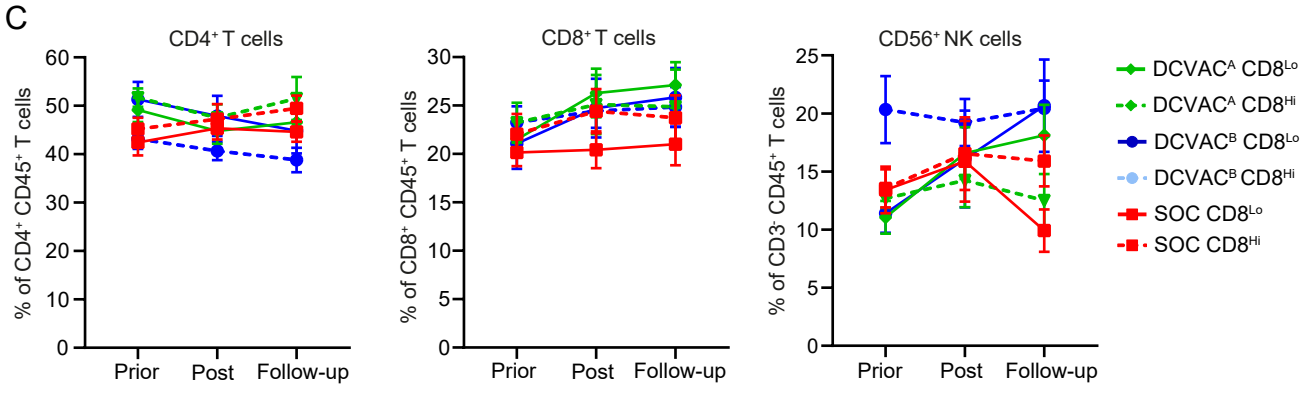

	DCVAC^A CD8^Lo	DCVAC^B CD8^Lo
SOC CD8^Lo	p=0.187	p=0.387
	DCVAC^A CD8^Hi	DCVAC^B CD8^Hi
SOC CD8^Hi	p=0.782	p=0.116

	DCVAC^A CD8^Lo	DCVAC^B CD8^Lo
SOC CD8^Lo	p=0.035	p=0.167
	DCVAC^A CD8^Hi	DCVAC^B CD8^Hi
SOC CD8^Hi	p=0.831	p=0.943

	DCVAC^A CD8^Lo	DCVAC^B CD8^Lo
SOC CD8^Lo	p=0.043	p=0.034
	DCVAC^A CD8^Hi	DCVAC^B CD8^Hi
SOC CD8^Hi	p=0.247	p=0.345

Figure 5

A

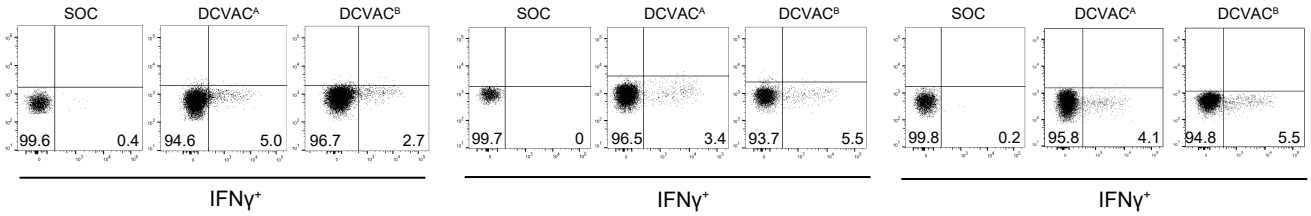

B

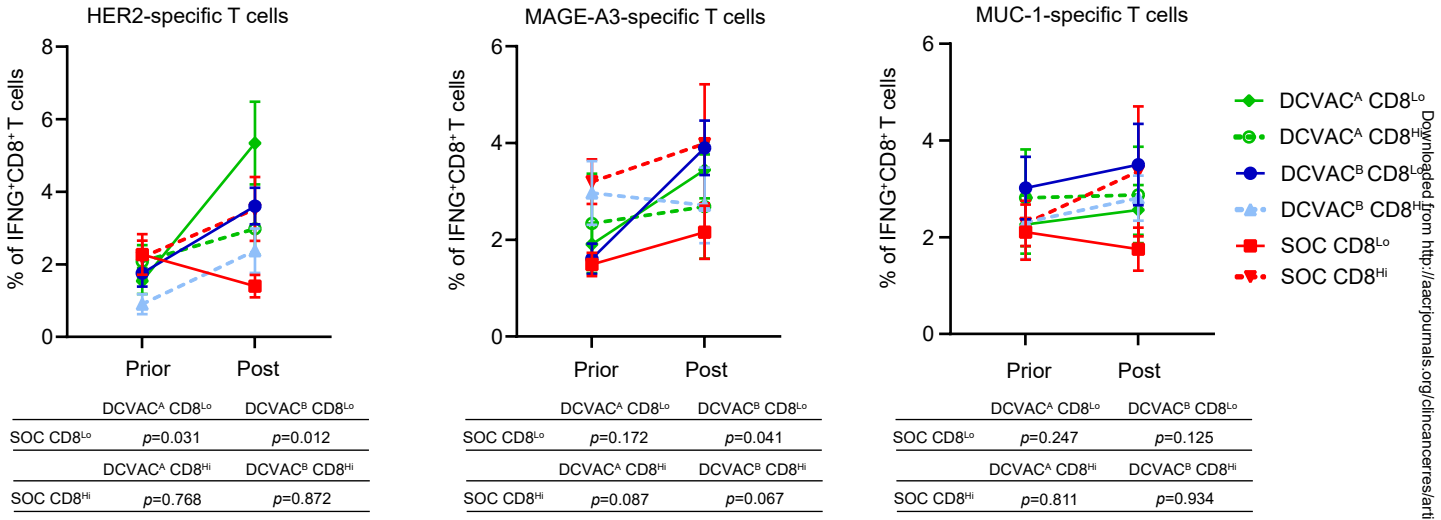

	DCVAC^A CD8^Lo	DCVAC^B CD8^Lo
SOC CD8^Lo	*p*=0.031	*p*=0.012
	DCVAC^A CD8^Hi	DCVAC^B CD8^Hi
SOC CD8^Hi	*p*=0.768	*p*=0.872

	DCVAC^A CD8^Lo	DCVAC^B CD8^Lo
SOC CD8^Lo	*p*=0.172	*p*=0.041
	DCVAC^A CD8^Hi	DCVAC^B CD8^Hi
SOC CD8^Hi	*p*=0.087	*p*=0.067

	DCVAC^A CD8^Lo	DCVAC^B CD8^Lo
SOC CD8^Lo	*p*=0.247	*p*=0.125
	DCVAC^A CD8^Hi	DCVAC^B CD8^Hi
SOC CD8^Hi	*p*=0.811	*p*=0.934

C

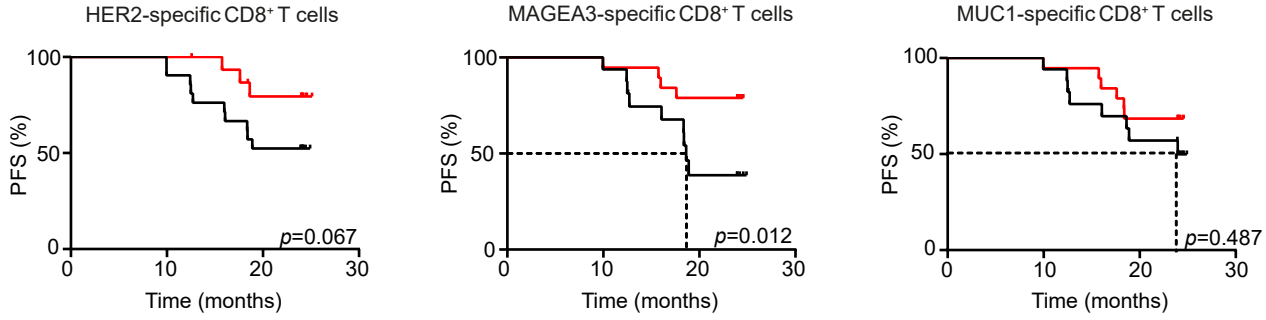

Time (months)	0	10	20	30
TAAs-CTL^Lo	19	18	11	1
TAAs-CTL^Hi	17	17	12	1

Time (months)	0	10	20	30
TAAs-CTL^Lo	17	17	5	1
TAAs-CTL^Hi	19	19	16	1

Time (months)	0	10	20	30
TAAs-CTL^Lo	17	16	9	1
TAAs-CTL^Hi	19	19	13	1